

## Synthesis of Gold Nanoparticles by Pulsed Laser Ablation and its Study Physical and Mechanical Properties

Ahmed Hamza Ahmed <sup>a</sup>, Awatif Saber Jasima <sup>a</sup>, and Saif Khalel Jasim <sup>b,\*</sup>

<sup>a</sup>.Department of Physics, College of Science, University of Tikrit, Tikrit, Iraq

<sup>b</sup>. Department of Radiology Techniques, Bilad Alrafidain University College, Diyala, 32001, Iraq

\*Corresponding author. Tel.: +0-000-000-0000; fax: +0-000-000-0000; e-mail:saifalaosy@gmail.com

Received 29 January 2024, Revised 7 March 2024, Accepted 22 April 2024

### ABSTRACT

In this work, the pulsed laser ablation technique was used, which is considered a good and distinctive method. Gold nanoparticles (AuNP) were prepared using an Nd-YAG laser with specific parameters, wavelength 1064 nm, constant ablation energy 1000 mJ, frequency 1 Hz, and different number of pulses (300, 600, and 900 pulse/sec). Deionized water was used as the medium liquid. The purpose of this study was to examine the change in these parameters on AuNP using a variety of Xrd, FESEM, Uv-Vis, force-hardness, and compression measurements. The pure cubic crystal structure of gold nanoparticles was analyzed using XRD. Subsequent FESEM images (average diameters 78.07nm, 49.15nm, 37.67nm) indicate that the particles had highly spherical and quasi-spherical shapes. Using ultraviolet analysis, the absorption band of gold nanoparticles was found and the wavelength was (518, 519, 524) nanometers, respectively. There were three different power gaps (1.895, 2.005, and 2.084) eV. In addition, mechanical property tests were conducted, where 2 ml of gold nanoparticles were mixed with (3 grams) of traditional dental filling. The hardness value increased by (3%). The results also showed an increase in the stress and strain value and an increase in Young's modulus. Hence, an increase in the compressive strength. This indicates that AuNP affects the mechanical properties and enhances their effectiveness.

**Keywords:** Laser, Ablation, Pulses, Filling, Au, SPR.

### 1. INTRODUCTION

Because nanomaterials have better physical and chemical properties than their bulk counterparts, their application has greatly expanded in a variety of industries, including electronics and medicine [1]. Particles in the condensed phase with sizes ranging from 1 to 100 nm are referred to as 'nanoparticles' (NP) [2]. NP are incredibly small in size and have a large surface area relative to their volume [3]. It has recently been demonstrated that the pulsed laser ablation in liquid medium (PLAL) method is a very effective tool for achieving the goal of changing the particle sizes of prepared nanostructured materials [4]. This method is based on the use of high-intensity pulsed laser ablation to create an interaction between the laser material, the target surface, and a plasma column that has been completely immersed in the liquid medium[5]. This circumstance creates unique thermodynamic conditions with high temperatures and pressures, enabling the production of very small molecules located at the nanoscale [6]. This arrangement can be used with different materials to create different shapes and sizes of nanostructured materials using the same techniques. This method can be considered an easy, affordable, and efficient way to synthesize various desired materials with a high degree of purity[7]. In addition, unlike other synthetic techniques, where potentially harmful contamination of the environment is prevented by fabricating nanostructured materials within the liquid path, for the reasons mentioned above, this technique is frequently used when examining the

effects of its effective parameters on particle sizes [8]. A variety of laser parameters including laser fluence, wavelength, pulse width, and irradiation time may be useful in PLAL screening of size-dependent prepared samples at the nanoscale [4]. The visible spectrum has unique optical properties of gold AuNP which result from the surface plasmon oscillation of free electrons induced by light [9]. When light is absorbed, this special property raises the temperature of the surrounding environment and has multiple uses [10]. The size, shape, and medium in which nanoparticles are found influence the colors they exhibit at the nanoscale. Due to their inert nature, durability, high contrast, non-toxicity, and compatibility, AuNP are widely used in biotechnology and biomedicine and have also been found to be the least toxic and safest agents for drug delivery [11, 12]. The production of gold nanoparticles can be enhanced simply by changing the laser wavelength, spot size, impact, pulse duration, repetition rate, and liquid medium [13-15].

### 2. MATERIAL AND METHODS

The target material was a gold (Au) plate with dimensions of (1 cm 1 cm and 2 mm) high and of high purity of about 99%. The target underwent cleaning and washing with ethanol followed by ten minutes in an ultrasonic acetone bath to remove impurities and then a

final rinse with distilled water. The target was placed inside a glass jar containing 5 ml of deionized water medium before ablation, after exposing the target to a vertical laser beam, a cavitation bubble was created as a result of intense pressure and fluid entrapment, in addition to a plasma column formed on its surface. This phenomenon occurred when a distance of 12 cm was determined between the laser-focusing lens and the refraction of light on the surface of the target material as explained based on Figure 1. Parameters related to a laser with a constant energy of 1000 mJ, operating at a frequency of 1 Hz, and the number of pulses (300, 600, and 900 pulse/sec) were used in the ablation process. Dental fillings were purchased from dental supply stores. The liquid containing gold nanoparticles was evaporated from 10 milliliters to 2 milliliters and kneaded with a dental filling. The filling was placed in special molds and then the filling was hardened using a UV machine.

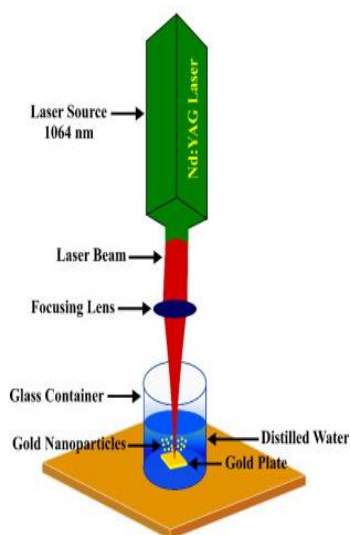


**Figure 1:** Schematic illustration of the pulsed laser ablation method.

Gold nanoparticles were prepared at room temperature after which the well-known drop casting method was used to prepare an AuNP film. Then measure the XRD of the membrane using a Bruker D2 Phase diffractometer; The scanning range was from 10° to 90° for 2θ and was plotted using Origin Lab 2023 software. Field emission scanning electron microscopy (FESEM) was used to study the morphology of the AuNP. The Image J program was used to calculate the size of the particle diameters, and the Origin Lab 2023 program was used to draw and analyze the results. The mechanical properties (hardness and

compressive strength) of the AuNP with dental fillings were also calculated and drawn using the Origin Lab 2023 program.

### 3. RESULTS AND DISCUSSION

#### 3.1. XRD ANALYSIS

Figure 2 shows the XRD pattern analysis view of an AuNP prepared using an optimized laser ablation sample prepared optimal sample at a pulse rate (900 pulse/sec). Miller index and full-width-half-width (FWHM) index were used to calculate crystallite size using Scherer's equation. Their XRD patterns are somewhat similar to those values in the ISBN (JCPDS 98-016-3723) and analysis has demonstrated that the particles are of the face-centered cubic type. The angles and grid parameters are ( $\alpha = \beta = \eta = 90^\circ$ ) and ( $a = b = c = 3.05$ ), respectively. Three peaks appear at angles 38.25, 44.51, and 64.79, as appears in (Table 1). These angles correspond to the (111), (002), and (022) directions, respectively, associated with the particle directions. No film was obtained for the samples prepared at 300 and 600 pulses due to the low concentrations prepared.

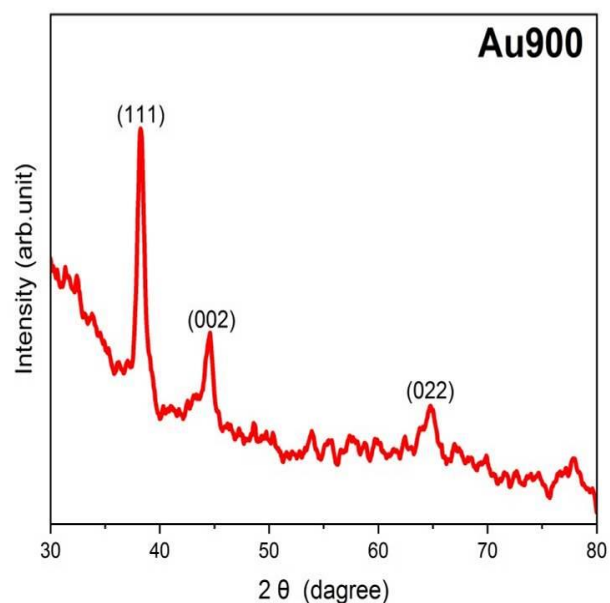


**Figure 2.** The XRD patterns of AuNP were produced at 900 pulse/sec.

**Table 1 .** Experimental and standard results of X-ray diffraction of AuNP

2θ (deg) Practical	2θ (deg) Standard	FWHM (deg)	crystalline size "D" (nm)	d <sub>hkl</sub> (Å) Practical	d <sub>hkl</sub> (Å) Standard	(hkl)	h <sup>2</sup> +k <sup>2</sup> +l <sup>2</sup>
38.24	38.26	0.2460	35.71	2.34	2.35	(111)	3
44.51	44.47	0.5904	15.19	2.02	2.03	(002)	4
64.74	64.71	1.1808	8.32	1.44	1.43	(022)	8

### 3.2. FESEM RESULTS

Figure 3 Indicates a view of FESEM measurements of AuNP at (300, 600, and 900) pulse/sec. AuNP has spherical and quasi-spherical shapes and these measurements show irregular geometric structures with

average diameters of 318.33, 202.76, and 159.12 nm, respectively. A decrease in average diameter was achieved as a result of reactive spraying which occurred as a result of increased pulsation. Table 2 indicates the results.

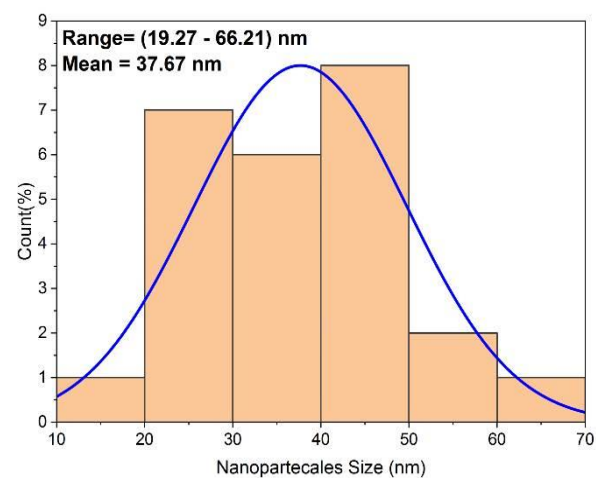
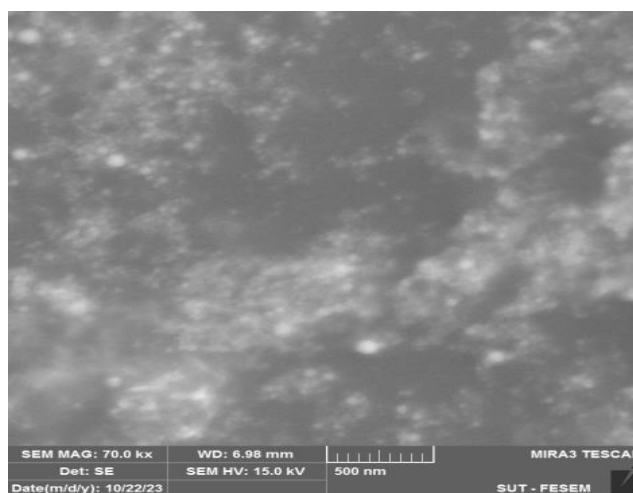
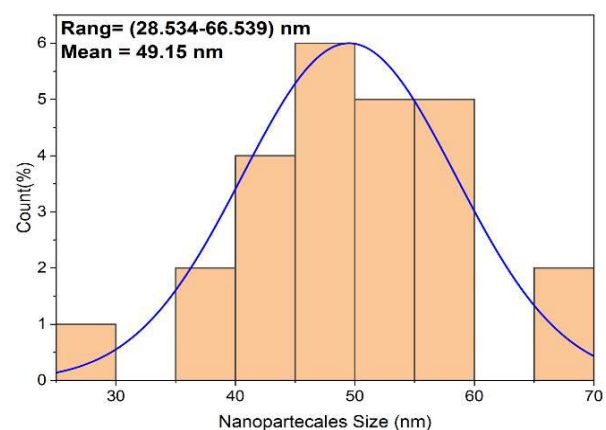
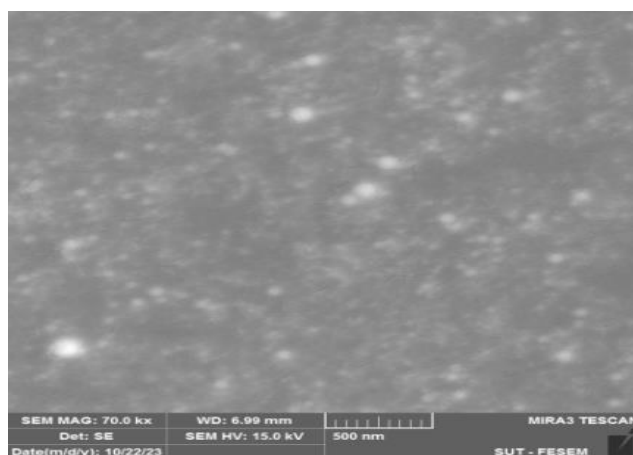
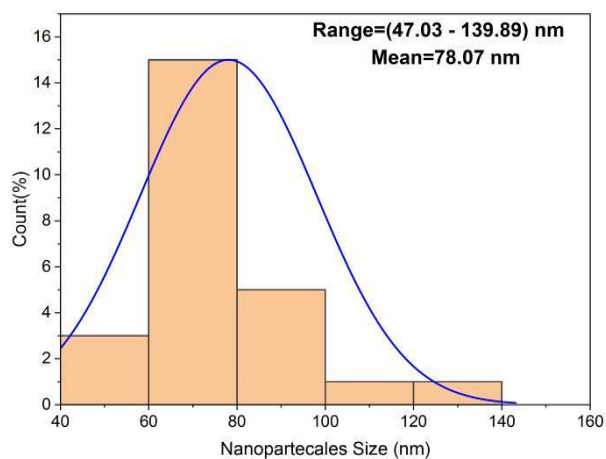
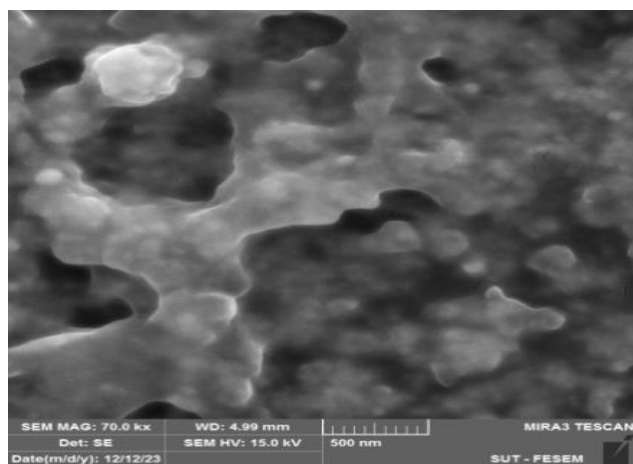


**Figure 3.** Result of FESEM at the number of pulses (300, 600, and 900 pulse/sec) for AuNP.

**Table 2.** The results of FESEM for AuNP at (300, 600, and 900) pulse/sec.

Pulses of number	Particle of shape	Average of size
300	Spherical	78.07 nm
600	Semi-spherical	49.15 nm
900	Spherical	37.67 nm

### 3.3. OPTICAL RESULTS

#### 3.3.1. UV-VIS SPECTRO

Figure 4. Interprets the results of the UV spectrum acquired by laser ablation of gold (Au) metal at different pulse numbers (300, 600, and 900 pulse/s) and constant energy. It also demonstrates that colloidal products are responsible for the nanoparticle's transmittance and UV-visible optical absorption spectra. A darker color indicates higher nanoparticle concentration. The intensity and repetition rate of laser pulses used for ablation have been shown to affect the position and width of the surface

plasmon resonance (SPR) absorption peak [12]. Moreover, the intensity of the SPR absorption peak increased with the internal color change relative to the number of pulses as it increased from 300 to 900 pulses per second. The high quantum confinement of AuNP is claimed to be responsible for the variable and higher absorption peak intensity. Since the ground state and excited state transitions require more energy due to the quantum confinement effect, smaller AuNP may have different absorption peaks [13]. Both the peak position and strength of the SPR absorption peak increased as they both showed a shift between (518, 519, and 524 nm). As the number of laser pulses increased, the absorption of AuNP increased to (0.158, 0.226, 0.243 IU), in this order.

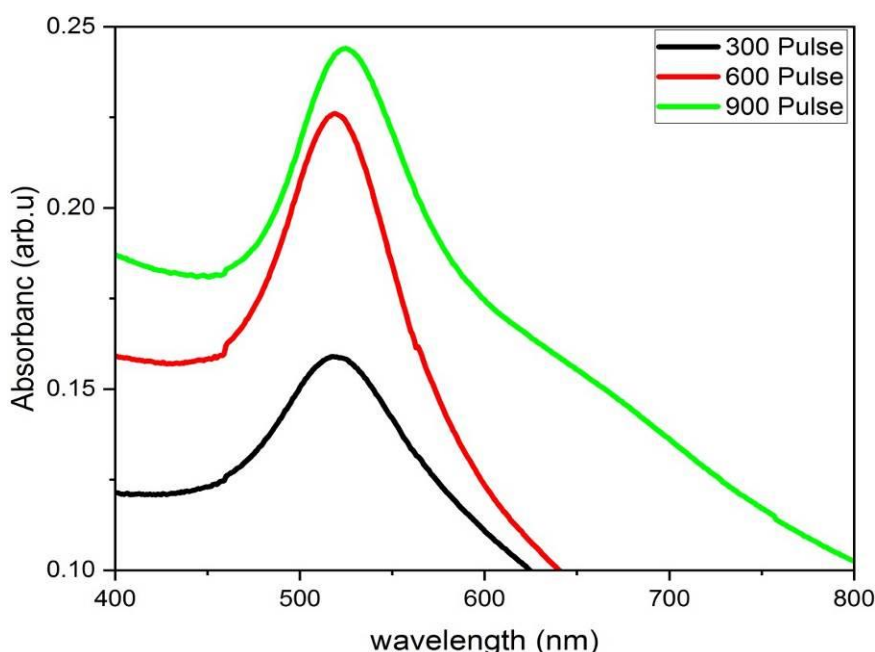


**Figure 4.** The results wavelength-dependent absorption of AuNP at 300, 600, and 900 pulse/sec.

#### 3.3.2. ENERGY GAP ANALYSIS

UV-visible absorption spectra can be used to calculate the energy gap directly or  $E_g$  (eV) using Einstein's photon energy equation.

$$E_g = hc / \lambda_{max} \dots\dots\dots (1)$$

Where  $\lambda_{max}$  is the maximum absorption wavelength,  $c$  is the speed of light, and  $h$  is Planck's constant. The following Tauc equation can also be used to determine the

conduction band energy of Au nanoparticles indirectly from their absorption spectra:

$$(\alpha hv)^2 = B(hv - E_g) \dots\dots\dots (2)$$

Where  $\alpha$  is the absorption coefficient,  $hv$  is the photon energy, and  $E_g$  is the energy gap. Equation (2), which plots  $(\alpha hv)^2$  versus  $(hv)$  and extrapolates the linear part of the curve to the energy axis, can be used to determine the energy gap range of nanoparticles [18,19]. Figure 5 indicates the energy gap of AuNP prepared at a number of pulses (300, 600, and 900 pulse/sec). The value of the



energy gap increases from 2.760 to 3.06 eV when the number of pulses increases, as clear in Figure 5. The energy gaps were 2.760 eV for the sample prepared at 300 pulses, 2.835 eV for the sample prepared at 600 pulses, and 3.06

eV for the sample prepared at 900. a beat. The sample with the highest number of pulses has the largest energy gap and the sample with the smallest number of pulses has the lowest energy gap; Their values are listed in Table (3).

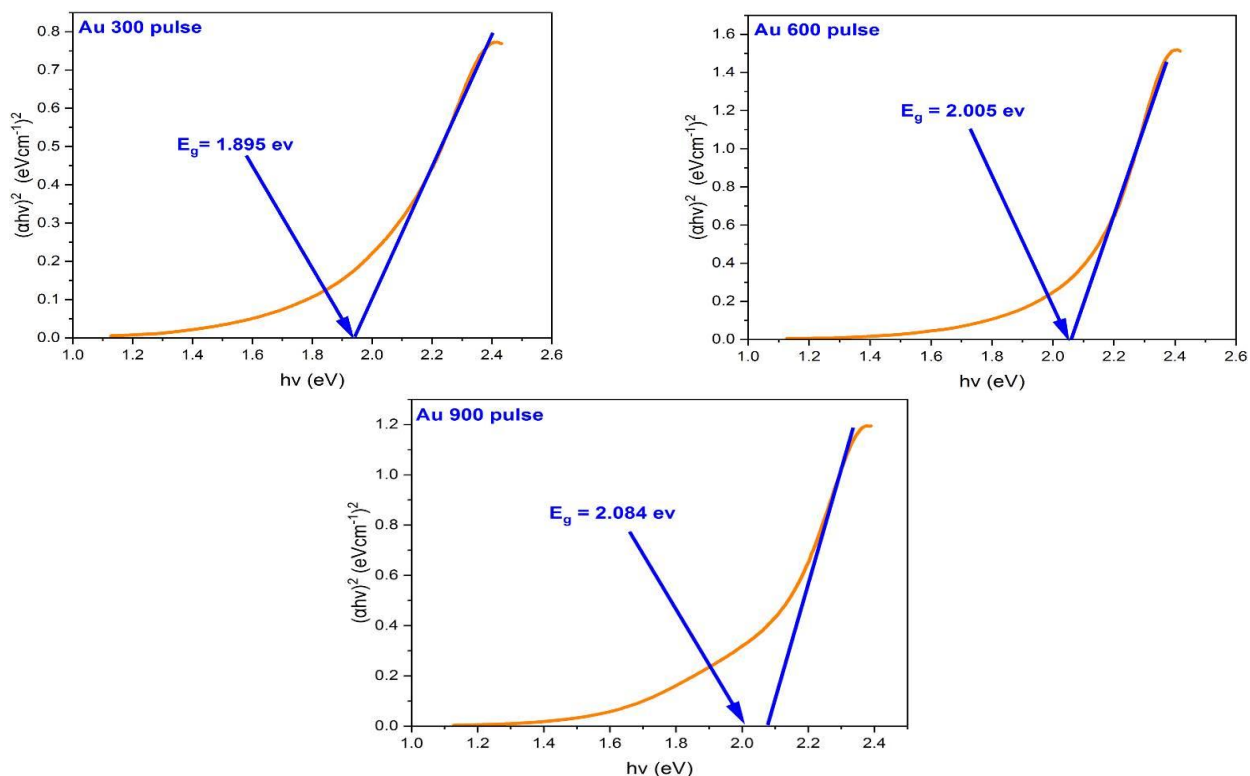


Figure 5. The energy gap for AuNP at (300, 600, and 900 pulse/sec).

Table 3. Demonstrates the energy gap values of AuNP in different pulses of numbers.

AuNP Pulses number (pulse/sec)	SPR (nm)	Eg (eV)
300	518	1.895
600	519	2.005
900	524	2.084

### 3.4. MECHANICAL PROPERTIES

The optimal sample prepared at a pulse rate of 900 pulse/sec was selected for mechanical testing (hardness and compressive strength). The liquid containing gold nanoparticles (10 mL to 2 mL) was evaporated at a temperature of 50 °C. The liquid was then combined with 3 grams of dental filling and a glass bowl was then placed over a heat source set at 50°C. The filling was then poured into special molds. The molds were cylindrical in shape, with a height twice the diameter, according to the American Society for Testing Materials ASTM (D2240)

standard [20]. It was treated with ultraviolet rays until it hardened. They were then removed from the mold for mechanical testing.

#### 3.4.1. HARDNESS

A durometer (Shore D) was used to measure the hardness of the samples and this requires a smooth and flat surface with a diameter larger than 30 mm. Diameter, depth, and distance from the edge more than 12mm all have a great influence on the hardness. The hardness tester is easy to use and works well and the tool can be easily removed to

enable this method[21]. Figure 6 indicates the results of the Shore D hardness test for pure dental filling samples at (84%) and dental fillings supported with gold nanoparticles at (87%). The highest value for the Shore D hardness measuring device is (100%). The results showed higher hardness values for the AuNP dental filling compared to the pure dental filling. The reason is that the hardness values will increase when AuNP is added to strengthen and reinforce the (pure) dental filling base material. The strength of materials increases as a result of their plastic deformation [22]. The resistance of dental filling composites needed to maintain interparticle alignment also increases with increasing concentrations of nanomaterials, which is also the reason for the increased hardness. For all these reasons, nanomaterials will eventually penetrate the matrix, enter the substrate and the matrix, and enter the spaces between them. This will ultimately result in a larger contact area which increases the contact and bonding between the nano-supported material and the pure dental filling. All this will strengthen the overlay layer and increase the hardness measurements. These results are almost consistent with the results of the researcher (Aly) [23]. Table 4 also explains the results.

**Table 4.** Hardness values for pure dental fillings with AuNP at 900 pulse/sec.

Simple	Hardness (Shore -D) MPa
Pure	84 %
Pure + Au NP	87 %

**3.4.2. COMPRESSIVE STRENGTH**

Compressive strength testing aims to confirm the behavior of the material or its response to pressure load. To do this, basic variables such as ductility and stress are measured. Compressive force is the amount of pressure needed to cause the sample to rupture under a compressive load during the chewing process where pressure is a major factor [24]. Figure 7 displays the stress-strain curves of the specimens: (a) pure dental filling. (b) AuNP-supported dental filling. The yield point is defined as one of the high points in the resistance of the body at which the material changes from a state of elastic deformation to plastic deformation [25]. From Figure 7, we notice that the yield point is less clear in the pure dental filling and clearer in the dental filling with AuNP due to the longitudinal fixation of the samples, where the samples are subjected to a load. The load was gradually increased until the sample was crushed, and due to the ability of AuNP to increase the surface area, we noticed an increase in the compressive strength by using dental fillings with gold nanoparticles. We also notice an increase in Young's modulus between pure dental fillings and dental fillings supported with gold nanoparticles [26]. Table 5 also displays the results.

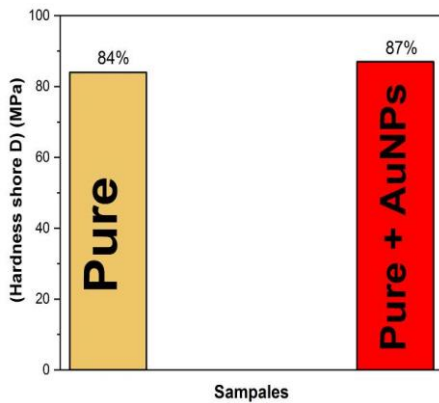


**Figure 6.** Hardness of dental filling with AuNP, number of pulses (900 pulse/sec).

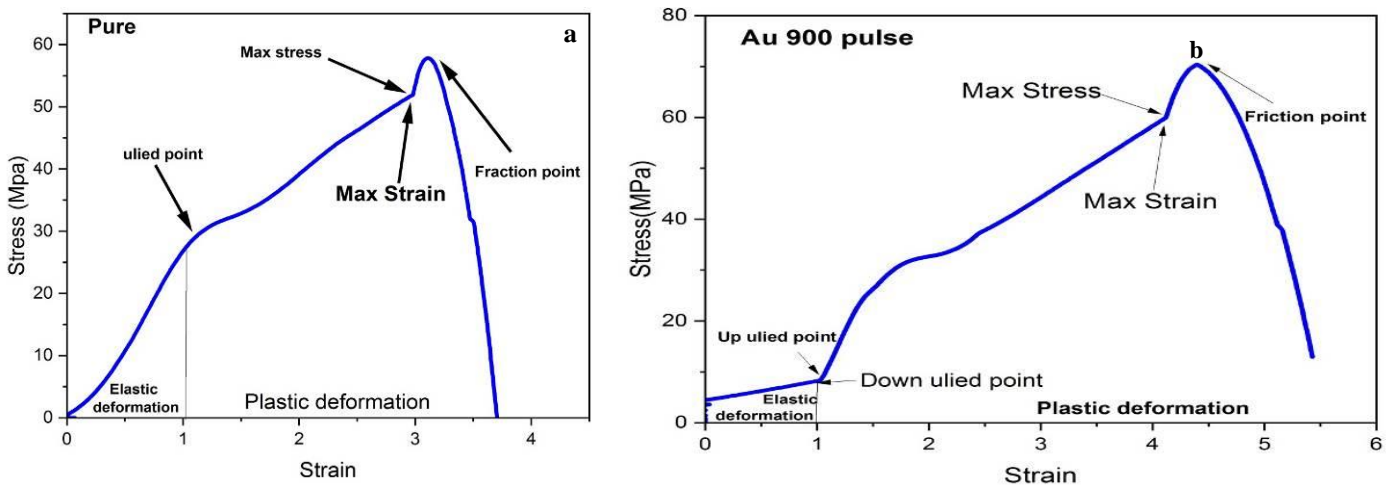


**Figure 7.** Displays Compressive strength value: (a) Pure dental filling. (b) Dental filling with AuNP.

**Table 5.** Young's modulus, maximum stress, and maximum strain for pure dental fillings and dental fillings with AuNP are presented.

Simple	Young's modulus N/mm <sup>2</sup>	Max stress N/mm <sup>2</sup>	Max strain
Pure	8.72	57.44	3.076
Pure+ AuNP	10.55	71.80	4.57

#### 4. CONCLUSION

In this study, a pulsed laser ablation technique in liquid was used with different pulse numbers in which spherical and colloidal AuNP were prepared in deionized water. Ultraviolet-visible (UV-Vis) analysis was one of the spectroscopic analytical techniques used to characterize NP synthesized in deionized water as well as XRD and FESEM examination as well as study of mechanical properties. The ultraviolet-visible (UV-Vis) results showed that there was an increase in the surface plasmon resonance with an increasing number of pulses and an increase in the energy gap with an increasing number of pulses. The FESEM results also showed a decrease in particle size with increasing number of pulses. The results of the mechanical properties showed an increase in the hardness between the pure dental filling and the dental filling with gold nanoparticles, as well as an increase in the compressive strength value. From this, we conclude that the preparation of gold nanoparticles can be used in biological and biomedical procedures as well as in developing the mechanical properties of dental fillings in a liquid medium possessing suitable optical properties.

#### ACKNOWLEDGEMENTS

The writers express their gratitude to the College of Science for granting permission to work in the college's laboratories.

#### REFERENCES

- [1] A. Nyabadza, M. Vazquez, B. Fitzpatrick, and D. Brabazon, "Effect of liquid medium and laser processing parameters on the fabrication of carbon nanoparticles via pulsed laser ablation in liquid towards paper electronics," *Colloids and Surfaces A: Physicochemical and Engineering Aspects*, vol. 636, p. 128151, 2022, doi: 10.1016/j.colsurfa.2022.128151.
- [2] S. Nakamura et al., "Synthesis and application of silver nanoparticles (Ag NP) for the prevention of infection in healthcare workers," *International Journal of Molecular Sciences*, vol. 20, no. 15, p. 3620, 2019, doi: 10.3390/ijms20153620.
- [3] A. S. Jasim, S. K. Jasim, and A. A. Habeeb, "Synthesis of Cinnamon Nanoparticles by Using Laser Ablation Technique," *Iraqi Journal of Physics*, vol. 19, no. 49, pp. 7-14, 2021, doi: 10.30723/ijp.v19i49.222.
- [4] A. M. Mostafa and E. A. Mwafy, "The effect of laser fluence for enhancing the antibacterial activity of NiO nanoparticles by pulsed laser ablation in liquid media," *Environmental Nanotechnology, Monitoring & Management*, vol. 14, p. 100382, 2020, doi: 10.1016/j.enmm.2020.100382.
- [5] A. H. Ahmed, A. S. Jasim, and S. K. Jasim, "Silver Oxid Nanoparticles Prepared by Pulsed Laser Ablation in Liquid and Their Study Physical Properties," *Web of Semantics: Journal of Interdisciplinary Science*, vol. 2, no. 2, pp. 1-9, 2024, doi: 10.1234/wos.v2i2.44.
- [6] R. C. Forsythe, C. P. Cox, M. K. Wilsey, and A. M. Muller, "Pulsed laser in liquids made nanomaterials for catalysis," *Chemical Reviews*, vol. 121, no. 13, pp. 7568-7637, 2021, doi: 10.1021/acs.chemrev.1c00007.
- [7] A. Subhan, A. H. I. Mourad, and Y. Al-Douri, "Influence of laser process parameters, liquid medium, and external field on the synthesis of colloidal metal nanoparticles using pulsed laser ablation in liquid: a review," *Nanomaterials*, vol. 12, no. 13, p. 2144, 2022, doi: 10.3390/nano12132144.
- [8] H. Du, V. Castaing, D. Guo, and B. Viana, "Rare-earths doped-nanoparticles prepared by pulsed laser ablation in liquids," *Ceramics International*, vol. 46, no. 16, pp. 26299-26308, 2020, doi: 10.1016/j.ceramint.2020.06.184.
- [9] S. N. Rashid and A. S. Jasim, "Effect of Nd: YAG laser on the optical properties of nanoparticle CuO solutions," *Materials Today: Proceedings*, vol. 80, pp. 3909-3912, 2023, doi: 10.1016/j.matpr.2023.04.532.
- [10] A. Rahman, A. Rahman, W. Ghann, H. G. Kang, and J. Uddin, "Terahertz multispectral imaging for the analysis of gold nanoparticles' size and the number of unit cells in comparison with other techniques," *International Journal of Biosensors & Bioelectronics*, vol. 4, pp. 159-164, 2018, doi: 10.15406/ijbsbe.2018.04.00088.
- [11] Y. J. Lee, E. Y. Ahn, and Y. Park, "Shape-dependent cytotoxicity and cellular uptake of gold nanoparticles synthesized using green tea extract," *Nanoscale Research Letters*, vol. 14, pp. 1-14, 2019.
- [12] M. Borzenkov, G. Chirico, M. Collini, and P. Pallavicini, "Gold nanoparticles for tissue engineering," *Environmental Nanotechnology: Volume 1*, pp. 343-390, 2018.
- [13] S. K. Jasim, A. S. Jasim, and A. A. Habeeb, "Growth Cinnamon Nanoparticles in Different Liquid by Pulsed Laser Ablation in Liquid PLAL," *MJPS*, vol. 8, no. 2, 2021.
- [14] K. Kalimuthu, B. S. Cha, S. Kim, and K. S. Park, "Eco-friendly synthesis and biomedical applications of gold nanoparticles: A review," *Microchemical Journal*, vol. 152, p. 104296, 2020.
- [15] T. Y. Sabri, S. K. Jasim, A. A. Habeeb, and A. S. Jasim, "Preparation and Study Ag Nanoparticles via PLAL Technique: Influence of Different Number of

- Pulses," *International Journal of Nanoelectronics and Materials (IJNeaM)*, vol. 17, no. 1, pp. 48-54, 2024.
- [16] P. Slepíčka et al., "Methods of gold and silver nanoparticles preparation," *Materials*, vol. 13, no. 1, p. 1, 2019.
- [17] A. A. Salim, S. K. Ghoshal, H. Bakhtiar, G. Krishnan, and H. H. J. Sapongi, "Pulse laser ablated growth of Au-Ag nanocolloids: Basic insight on physiochemical attributes," *Journal of Physics: Conference Series*, vol. 1484, no. 1, p. 012011, 2020.
- [18] S. Hathwara, B. L. Devi, and D. Ramananda, "Optical and Dielectric Properties of Poly (Vinyl Pyrrolidone-co-Vinyl Acetate)-Capped ZnS Nanoparticles," *Journal of Electronic Materials*, vol. 50, no. 8, pp. 5007-5012, 2021.
- [19] M. Skiba, V. Vorobyova, and O. Pasenko, "Surface modification of titanium dioxide with silver nanoparticles for application in photocatalysis," *Applied Nanoscience*, vol. 12, no. 4, pp. 1175-1182, 2022.
- [20] S. I. Salih, W. M. Salih, and T. A. Mohameed, "Investigation of Some Mechanical Properties of Ternary Polymer Blends Based on Polypropylene," 2022.
- [21] W. D. Callister Jr., *Materials Science and Engineering: An Introduction*, 7th ed., 2007.
- [22] I. W. Watan, "Studying some of the mechanical & thermal properties of polyester reinforced with ceramic particles," *Diyala Journal of Human Research*, no. 37, 2009.
- [23] A. A. Aly, M. M. Mahmoud, and A. A. Omar, "Enhancement in mechanical properties of polystyrene filled with carbon nano-particulates (CNPs)," *World Journal of Nano Science and Engineering*, vol. 2, no. 2, pp. 103-110, 2012.
- [24] A. J. Jefferson, V. Arumugam, and H. N. Dhakal, *Repair of Polymer Composites: Methodology, Techniques, and Challenges*, Woodhead Publishing, 2018.
- [25] M. S. Rao and P. S. V. Narayana, "Preparation And Characterization Of A Novel Natural Fiber Based Composite For Dental Implants," *Journal of Pharmaceutical Negative Results*, pp. 2108-2120, 2023.
- [26] H. Nasiri, A. Homafar, and S. C. Chelgani, "Prediction of uniaxial compressive strength and modulus of elasticity for Travertine samples using an explainable artificial intelligence," *Results in Geophysical Sciences*, vol. 8, p. 100034, 2021.